

The Welding Deformations of Chrome-nickel Stainless Steels

M. Audronis*, J. Bendikas

Materials Science and Welding Department, Vilnius Gediminas Technical University,
Basanavičiaus 28, LT-2009 Vilnius, Lithuania

Received 02 May 2002; accepted 23 May 2003

Stainless steels are widely used for manufacturing important constructions. Because of their properties, welding deformations of stainless steels are larger than those of mild steels. Therefore it is important to foresee forthcoming welding deformations and their extent.

Welding deformations are often calculated using analytical approaches or finite element analysis. In this article the methodologies of Okerblom, Walter, Horst Pflug, Sparagen – Ettinger, Blodgett and finite element analysis, were applied to calculate deformations. The experimental study of deformations was made using austenitic stainless steel X8CrNiTi 18-10. The results of analytic analysis were compared with the results of the experimental analysis.

Keywords: stainless steels, welding deformations, finite element analysis.

INTRODUCTION

In the recent time the strength, durability, accuracy of assembly etc. requirements for welded constructions are increasing [1–3]. This especially involves important constructions and parts, which are often made of chrome-nickel stainless steels. The most widely used steel is the austenitic chrome-nickel stainless steels stabilized with titanium.

The properties of these steels (Table 1) give large welding deformations and this reduces strength and durability, and inconveniences in assembling operations. Therefore it is important to foresee forthcoming welding deformations and their extent.

Welding deformations are often calculated using analytical approaches [1, 2]; finite element analysis (FEA), which in almost all cases is performed using sequential coupled-field analysis, is widely used too [4–9], but there are still many controversial questions related to modeling of moving electric arc; evaluation of the final temperature of welding bath and the latent heat of melting; solidification of welding bath and the corresponding latent heat; thermal dilatation, inelastic deformation and residual stresses evolution during cooling; thermal boundary conditions including convection, radiation, and conduction as well as the thermal contact resistance of a basement [10–12]. And also, the sequential coupled-field analysis requires not inconsiderable time. Different analytical approaches give great dispersion of the results and different conformity with experimental results. Therefore the objectives of this study were to determine which approaches give most accurate results for calculation of stainless steels welding deformations and to create authentic finite element model to predict residual displacements of these steels during tungsten inert gas (TIG) welding, using the faster - direct method of coupled-field analysis.

The methods of Okerblom, Walter, Horst Pflug, Sparagen – Ettinger, Blodgett [2] or finite element analysis

were applied to calculate deformations. Calculation results were compared between themselves and with the experimental analysis results.

EXPERIMENTAL ANALYSIS

Experimental analysis of stainless steel welding deformations was made using samples shown in Fig. 1. For this purpose the X8CrNiTi 18-10 (EN 10027) stainless steel was used.

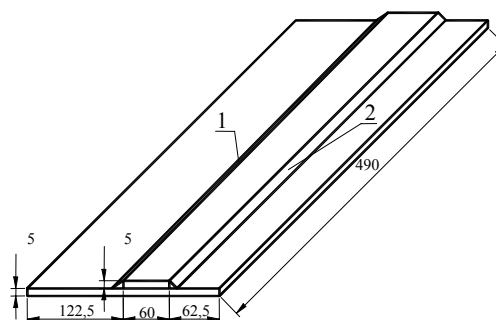


Fig. 1. The shape and dimensions (in millimeters) of welded samples (1 and 2 indicates the sequence of welds)

Before welding, the plates were carefully cleaned and tack welded. Then initial measurements in marked points of the sample (see Fig. 2 in [14]) were taken [13, 14]. Analogous measurements in the same points were taken having welded the first and the second welds and after complete cooling each time. The displacements of marked points were measured with indicators (the partition value - 0.01 mm). Having processed the measurement results, all deformation types of the sample were determined. They are: longitudinal contraction, longitudinal deflection, deflection on the plate's plane, transversal contraction and transversal deflection. The samples were welded by TIG welding. The welding parameters are listed in Table 2.

Experimental analysis shows that the smallest longitudinal deflection and deflection on the plate's plane have the samples No.1 and No.2; the smallest transversal contraction – No.1, the biggest – No.3; the smallest longitudinal contraction have sample No.3; the smallest

* Corresponding author. Tel.: +370-5-2744739; fax.: +370-5-2744739.
E-mail address: martynas.audronis@me.vtu.lt (M. Audronis)

Table 1. The physical properties of X8CrNiTi 18-10 steel (EN 10027)

Material	CTE, linear $\alpha \times 10^6$ 1/K	Thermal conductivity λ , W/m·K	Heat capacity $c\gamma$, J/cm ³ K	Heat conductivity α , cm ² /s
X8CrNiTi 18-10 (EN 10027)	18	28	4.6	0.06

Table 2. The welding parameters of samples

Sample	I_w , A	U_{arc} , V	Welding speed, cm/s	Number of runs	Filler metal
No. 1	180	18	0.417	1	-
No. 2	180	18	0.417	1	+
No. 3	140	14	0.694	2	+

transversal deflection – sample No.1 The experimental analysis results, together with the calculations and finite element analysis results, are given in Table 3. In the issue it's true to say that the sample No.1 had the smallest deformations overall and its welding parameters were most optimal in this case.

CALCULATION METHODS, ANALYSIS AND RESULTS

The transverse and longitudinal contraction, deflection, and deflection on the plate's plane were calculated accordingly to before-mentioned welding deformations calculation methods that are stated below. All methods are taken from [2].

The purpose of all methods is the same - to calculate welding strains, and the approaches are similar. The main differences are the estimation of input line energy and the physical properties of material.

The relation between the line energy and weld parameters is given by Eq. (1):

$$Q = \frac{UI\eta}{v}, \quad (1)$$

where U is the voltage, I is the current, v is the welding speed and η is an arc efficiency.

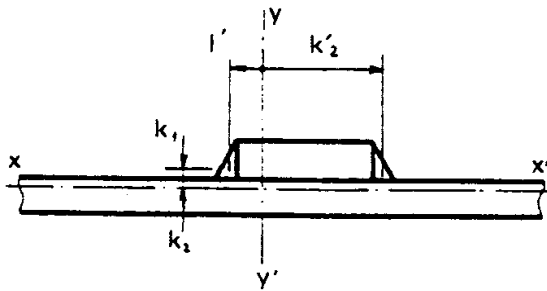


Fig. 2. The arrangement of neutral axes; k_1, k_2, k_1', k_2' – distances to the neutral axes

Calculation of the longitudinal contraction according to Okerblom:

Deformations after welding first and second welds:

$$\varepsilon_1 = -0.355 \frac{\alpha}{c} q_1 \frac{1}{S}, \quad (2)$$

$$\frac{\varepsilon_{1+2}}{\varepsilon_1} = 1 + \frac{q_2}{q_1} \frac{\sigma + 1}{\sigma - 0.693}, \quad (3)$$

here

$$\sigma = \frac{\frac{\sigma_t}{E} cS}{0.335\alpha q_1} \frac{1}{1 + \frac{k_2}{k_1} \frac{k_1^2 S}{J_x}}; \quad (4)$$

q_1, q_2 is the line energy for the first and second welds; α is the coefficient of linear expansion; c is the specific heat; S is the area of sample cross-section; σ_t is the yield strength; E is the Young's modulus; J_x is the moment of inertia of cross-section; L is the length of the weld.

Longitudinal contraction:

$$\Delta_L = \varepsilon_{1+2} L \quad (5)$$

Calculation of the longitudinal contraction after the first weld according to Walter is the same as stated in (2). Calculation of the longitudinal contraction after the second weld is given by Eq. (6).

$$\frac{\varepsilon_{1+2}}{\varepsilon_1} = 1 + \frac{q_2}{q_1} \frac{\sigma + 1}{\sigma - 0.693} \frac{1 - \frac{k_2}{k_1}}{1 + \frac{k_1^2 S}{J_x}} \frac{\sigma_0 + d}{\sigma_0 + 1}, \quad (6)$$

here

$$\sigma_0 = \frac{\frac{\sigma_t}{E} cS}{0.335\alpha q_1} \frac{1}{1 + \frac{k_1^2 S}{J_x}}; \quad (8)$$

Calculation of the longitudinal contraction according to Sparagen and Ettinger:

$$\Delta_L = 0.025 \frac{s_0}{S} L, \quad (9)$$

here s_0 is the cross-section area of the weld.

Calculation of the longitudinal contraction according to Horst Pflug:

$$\Delta_L = \frac{42\sigma_t}{E} \frac{s_0}{(S - s_0)} L. \quad (10)$$

Calculation of the longitudinal deflection according to Okerblom:

Deformations after welding first and second welds:

$$\frac{1}{p_1} = -0.355 \frac{\alpha}{c} q_1 \frac{k_1}{J_x}; \quad (11)$$

$$\frac{p_1}{p_{1+2}} = 1 + \frac{q_2}{q_1} \frac{k_1}{k_2} \frac{\sigma + 1}{\sigma - 0.693}. \quad (12)$$

Deflection of the sample:

$$f = \frac{1}{p_{1+2}} \frac{L^2}{8}. \quad (13)$$

Calculation of the longitudinal deflection after the first weld according to Walter is the same as stated in (11). Calculation of the longitudinal deflection after the second weld is given by Eq. (15).

$$\frac{p_1}{p_{1+2}} = 1 + \frac{q_2}{q_1} \frac{k_1}{k_2} \frac{\sigma + 1}{\sigma - 0.693} \left[1 - \frac{1 + \frac{k_2}{k_1} \frac{k_1^2 S}{J_x}}{(\sigma_0 + 1) \frac{k_1}{k_2} \left(1 + \frac{k_1^2 S}{J_x} \right)} \right], \quad (14)$$

Calculation of the longitudinal deflection according to Blodgett:

$$f = 0.005 \frac{s_0 k_1 L^2}{J_x}. \quad (15)$$

Calculation of the longitudinal deflection according to Horst Pflug:

$$f = \frac{42 s_0 k_1 L^2}{8 E J_x}. \quad (16)$$

Calculation of the deflection on the plate's plane according to Okerblom:

$$\frac{1}{p_1} = -0.355 \frac{\alpha}{c} q_1 \frac{k_1'}{J_y}; \quad (17)$$

$$\frac{p_1}{p_{1+2}} = 1 + \frac{q_2}{q_1} \frac{k_1'}{k_2'} \frac{\sigma + 1}{\sigma - 0.693}, \quad (18)$$

$$\text{here } \sigma = \frac{\frac{\sigma_t}{E} c S}{0.335 \alpha q_1} \frac{1}{1 + \frac{k_2'}{k_1'} \frac{k_1'^2 S}{J_y}}; \quad (19)$$

Calculation of the deflection on the plate's plane after the first weld according to Walter is the same as stated in (17). Calculation of the longitudinal deflection after the second weld is given by Eq. (20):

$$\frac{p_1}{p_{1+2}} = 1 + \frac{q_2}{q_1} \frac{k_1'}{k_2'} \frac{\sigma + 1}{\sigma - 0.693} \left[1 - \frac{1 + \frac{k_2'}{k_1'} \frac{k_1'^2 S}{J_y}}{(\sigma_0 + 1) \frac{k_1'}{k_2'} \left(1 + \frac{k_1'^2 S}{J_y} \right)} \right] \quad (20)$$

$$\text{here } \sigma_0 = \frac{\frac{\sigma_t}{E} c S}{0.335 \alpha q_1} \times \frac{1}{1 + \frac{k_1'^2 S}{J_y}}; \quad (21)$$

Calculation of the deflection on the plate's plane according to Blodgett:

$$f = 0.005 \frac{s_0 k_1' L^2}{J_y}. \quad (22)$$

Calculation of the deflection on the plate's plane according to Horst Pflug:

$$f = \frac{42 s_0 (k_2' - k_1') L^2}{8 E J_y}. \quad (23)$$

Calculation of the transversal contraction according to Sparagen and Ettinger:

$$\Delta_{sk} = 1,016 \frac{k}{h}, \quad (24)$$

here k is the pale and h is the thickness of the plate.

As we see all the methods take into account mechanical properties and geometrical characteristics of the sample's shape and position of the welds and only Okerblom and Walter takes into account physical properties of the material and input line energy.

The results of calculations according to the different methods differ greatly (Table 3). This comparison allows determining, which methodology lets to calculate welding deformations of chrome-nickel stainless steels most accurate.

FINITE ELEMENT ANALYSIS

Nonlinear thermal loading cycles produce nonlinear thermal strains which result in residual stresses and strains after welding and their effects on welded structures cannot be disregarded. Because of this the determination of residual stresses and strains in welded structures is an essential task.

Because of experimental researches require many time and are costly, the finite element analysis is applied to calculate welding deformations more and more often [4 – 16]. Comparison of finite element analysis results with experimental analysis results allows to determine if chosen model is proper and how accurate results does it gives.

Performing finite element analysis two models of sample No. 1 were applied: two dimensional, which was intended for transversal deformations calculation (Fig. 3) and three dimensional (Fig. 4).

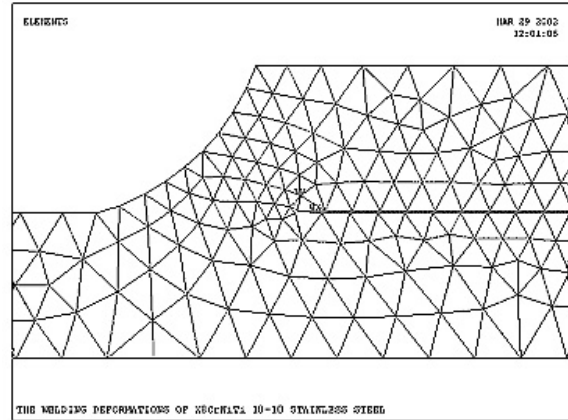


Fig. 3. The fragment of sample's No.1 2D model

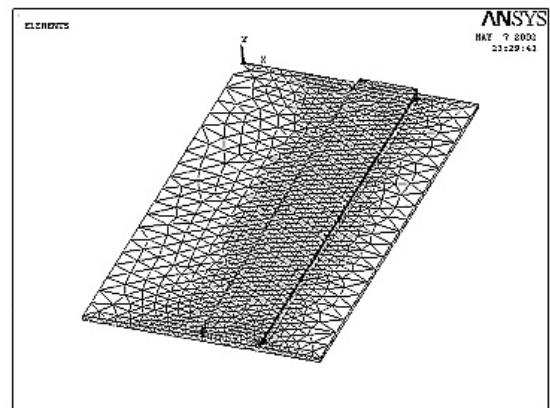


Fig. 4. Sample's No.1 3D model

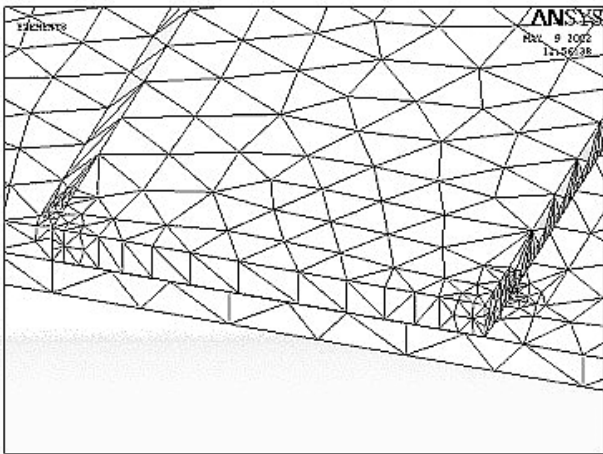


Fig. 5. First weld and tack welding

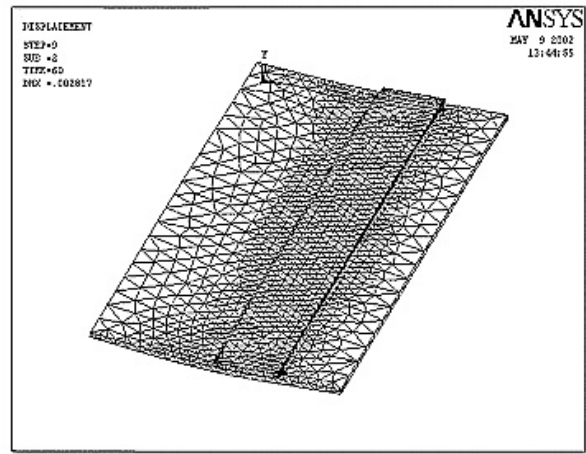


Fig. 7. A displacement after the first weld was welded

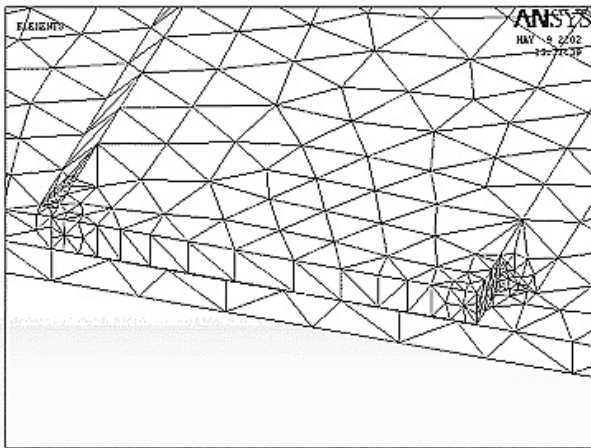


Fig. 6. The first and the second welds

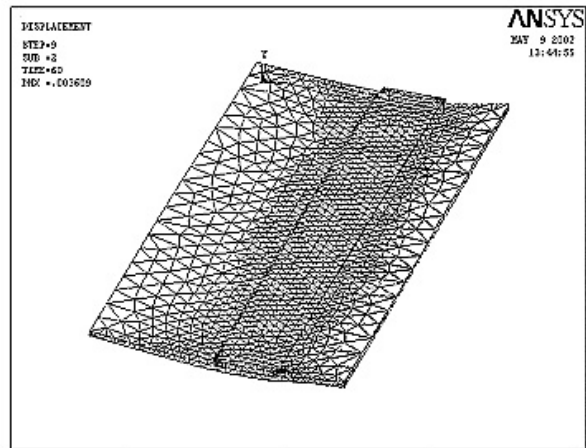


Fig. 8. A displacement after the second weld was welded

Table 3. The results of analytical and experimental analysis of welding deformations of X8CrNiTi 18-10 steel

Sample No.	Deformation	Experimental analysis	Okerblom	Walter	Sparagen-Ettinger	Blodgett	Horst Pflug	Finite element analysis using 2D model	Finite element analysis using 3D model
1	Longitudinal contraction, mm	0.44	0.74	0.30	0.27	–	0.42	–	0.14
2		0.50	0.76	0.61	0.42	–	0.65	–	–
3		0.22	0.49	0.42	0.32	–	0.50	–	–
1	Longitudinal deflection, mm	3.08	9.35	12.14	–	3.37	6.45	–	1.78
2		3.02	11.70	9.49	–	5.16	9.86	–	–
3		3.96	7.61	6.55	–	3.97	7.58	–	–
1	Deflection on the plates plane, mm	0.09	0.27	0.27	–	0.15	0.29	–	0.023
2		0.17	0.28	0.27	–	0.23	0.45	–	–
3		0.42	0.20	0.19	–	0.36	0.34	–	–
1	Transversal contraction, mm	0.46	–	–	0.91	–	–	0.16	0.11
2		0.55	–	–	1.02	–	–	0.17	–
3		0.66	–	–	1.24	–	–	–	–
1	Transversal deflection, mm	4.56	–	–	–	–	–	3.22	2.41
2		4.68	–	–	–	–	–	3.39	–
3		5.62	–	–	–	–	–	–	–

The calculation of residual stresses and strains using FEA is often performed using sequential coupled-field analysis, which algorithm is widely known, used and published [4, 7, 14]. The essence of the sequential method is that it involves two or more sequential analyses, each belonging to a different field. You couple the two fields by applying results from the first analysis as loads for the second analysis. Such type analysis is a sequential thermal-stress analysis where nodal temperatures from the thermal analysis are applied as "body force" loads in the subsequent stress-strain analysis.

However sequential coupled-field analysis requires not inconsiderable time. In our study we have used direct method of coupled-field analysis, which is faster, especially when the analysis consists of many steps. This method involves just one analysis that uses a coupled-field element type containing all necessary degrees of freedom. Coupling is handled by calculating element matrices or element load vectors that contain all necessary terms.

To create the welded structures models PLANE13 and SOLID98 finite elements for 2D and 3D models accordingly were used. The finite element model was fixed in the points as during real experiment. The steel studied is the isotropic, plastic material. It was taken the view, that the weld was welded momentarily in all length. The weld sequence, tack welding (Fig. 5, 6), strain hardening, physical and mechanical properties that depend on temperature [17] were considered.

The results of finite element analysis show, that calculating transversal deflection and contraction 2D model gives more accurate, but still imperfect results. The reason of poor results of both analyses is short information on material's properties that depend on temperature. Of course, presumption that the weld was welded momentarily in all length, decreases 3D model's accuracy too, therefore additional analysis, in which the weld should be filled step by step, is necessary.

The results of finite element analysis using 3D model are illustrated by Figures 7 and 8. They show displacements after welding first and second welds, accordingly.

CONCLUSIONS

1. The welding deformations calculation methods of Okerblom, Walter, Horst Pflug, Sparagen – Ettinger and Blodgett, applied to calculate deformations of welded samples, give the results that differ greatly.

2. Calculating the longitudinal contraction the best conformity with the experimental results is given by the method of Sparagen – Ettinger; calculating the longitudinal deflection and deflection in the plate's plane, the best conformity with the experimental results is given by the method of Blodgett.

3. Sample No. 1 (welded with 180A welding current, 0.417 cm/s welding speed and without filler metal) had smallest deformations overall and its welding parameters were most optimal in that case.

4. The finite element analysis using both 2D and 3D models gives imperfect accuracy results. The reason of poor results of both analyses is short information on material properties that depend on temperature. Presumption that the weld was welded momentarily in all length, decreases 3D model's accuracy too, therefore

additional analysis, where the weld should be filled step by step, is necessary.

REFERENCES

1. **Vinokurov, V. A., Grigoriānc, A. G.** Theory of Welding Deformations and Stresses. Moscow, Mechanical Engineering, 1984: 280 p. (in Russian).
2. **Gerbeaux, H., Piette, M., Renault, J-P.** Deformations and Stresses in Welding. Paris: Publications de la Soudure Autogene, 1988: 108 p. (in French).
3. **Puchaicela, T.** Welded Steel Constructions Deformations Control *Welding Journal* 8 1998: pp. 49 – 52 (in Russian).
4. **Teng, T. L., Chang, P. H.** A Study of Residual Stresses in Multi-pass Girth-butt Welded Pipes *Int. J. Pres. Ves. & Piping* 74 1997: pp. 59 – 70.
5. **Brickstad, B., Josefson, B. L.** A Parametric Study of Residual Stresses in Multi-pass Butt Welded Stainless Steel Pipes *Int. J. Pres. Ves. & Piping* 75 1998: pp. 11 – 25.
6. **Bachorski, A., Painter, M. J., Smailes, A. J., Wahab, M. A.** Finite Element Prediction of Distortion during Gas Metal Arc Welding Using the Shrinkage Volume Approach *Journal of Materials Processing Technology* 92 – 93 1999: pp. 405 – 409.
7. **Teng, T. L., Chang, P. H., Ko, H.C.** Finite Element Analysis of Circular Patch Welds *Int. J. Pres. Ves. & Piping* 77 2000: pp. 643 – 650.
8. **Wen, S. W., Hilton, P., Farrugia, D. C. J.** Finite Element Modeling of a Submerged Arc Welding Process *Journal of Materials Processing Technology* 119 2001: pp. 203 – 209.
9. **Zhu, X. K., Chao, Y. J.** Effects of Temperature Dependent Material Properties on Welding Simulation *Computers & Structures* 80 2002: pp. 967 – 976.
10. **Ronda, J., Oliver, G. J.** Comparison of Applicability of Various Thermo-viscoplastic Constitutive Models in Modeling of Welding *Comput. Methods Appl. Mech. Engrg.* 153 1998: pp. 195 – 221.
11. **Ronda, J., Oliver, G. J.** Consistent Thermo-mechano-Metallurgical Model of Welded Steel with Undefined Approach to Derivation of Phase Evolution Laws and Transformation-induced Plasticity *Comput. Methods Appl. Mech. Engrg.* 189 2000: pp. 361 – 417.
12. **Sarkani, S., Tritchkov, V., Michaelov, G.** An Efficient Approach for Computing Residual Stresses in Welded Joints *Finite Elements in Analysis and Design* 35 2000: pp. 247 – 268.
13. **Audronis, M., Bendikas, J., Visniakas, I.** The Comparison of Chrome-nickel Stainless Steel Welding Deformations Estimation by Different Methodologies *Proceedings of 5th Conference of Young Lithuania Researchers, Vilnius, Lithuania*, 2002: pp. 149 – 154 (in Lithuanian).
14. **Vishniakov, N., Cernasejus, O., Bendikas, J.** The 08X18H10T Stainless Steel Constructions Stress and Strain Estimation after Multi-pass Welding *Materials Science (Medžiagotyra)* 8 (1) 2002: pp. 20 – 25.
15. **Medvedev, S. V.** The Computer Modeling of Residual Welding Deformations Beside Technological Designing of Welded Constructions *Welding Fabrication* 8 (801) 2001: pp. 10 – 18 (in Russian).
16. **Barauskas, R.** Basics of the Finite Element Method. Kaunas, Technologija, 1998: 376 p. (in Lithuanian).
17. **Poluhin, L. I., Gun, G. J., Galkin, A. M.** Stand of Metals and Alloys for Plastic Deformation. Moscow, Metallurgy, 1983: 352 p. (in Russian).